

## Self-consistent solution of Galitskii-Feynman equations at finite temperature

P. Bożek\*

*National Superconducting Cyclotron Laboratory, and Department of Physics and Astronomy, Michigan State University,  
East Lansing, Michigan 48824*

*and Institute of Nuclear Physics, PL-31-342 Kraków, Poland*

(Received 18 November 1998)

We solve the in-medium  $T$ -matrix equation at finite temperature including the off-shell propagation of nucleons. In this way a self-consistent spectral function for the nucleons is obtained. The results are compared to a calculation using the quasiparticle approximation in the  $T$ -matrix equation. Also the effective in-medium cross sections for the two cases are compared. [S0556-2813(99)03805-4]

PACS number(s): 24.10.Cn, 21.65.+f

### I. INTRODUCTION

The calculation of properties of a strongly interacting many-body system is a challenging problem. Many efforts have been devoted to calculations of the nuclear matter properties, both at zero and at finite temperature. Most of those studies have been restricted to the quasiparticle approximation. The quasiparticle approximation can be justified in the vicinity of the Fermi energy at zero temperature [1]. Explicit calculation shows that the width of the spectral function approaches zero when the energy approaches the Fermi energy and the temperature tends to zero [2,3]. However, the knowledge of the whole spectral function is needed for a self-consistent Brueckner or Galitskii-Feynman calculation. Moreover at larger temperatures there is no region in the momentum space where the Pauli blocking reduces the scattering width. If one wants to address the dynamics of heavy-ion collisions at energies of a few hundreds of MeV per nucleon the knowledge of effective cross sections in dense and excited nuclear matter is needed. The calculation of the in-medium  $T$  matrix (or the Brueckner  $G$  matrix) gives an estimate of this cross section [4]. The calculation of the in-medium cross section (at equilibrium) can and should take into account the off-shell propagation of the nucleons. The off-shell propagation of scattering nucleons changes quantitatively the value of the cross section and in the case of soft emission it changes also its qualitative behavior [5,6].

The existing calculations of the nuclear spectral functions assume a quasiparticle approximations in the summation of the ladder diagrams [7,2,8,3,9–11]. From the knowledge of the  $T$  matrix (in the Galitskii-Feynman equations) or the  $G$  matrix (in the Brueckner equations) the imaginary part of the one-particle self-energy can be calculated [12–14]. However, it has been noted already several years ago that calculations of the self-energy in the Born approximation using a semiclassical collision term and a quantum collision term with off-shell propagators give different results [15]. The semiclassical one-particle width being generally larger than the self-consistent quantum one. Clearly the spectral functions obtained in the quasiparticle approximation should be

checked in a self-consistent calculation with in-medium off-shell nucleon propagators.

A spectral function obtained in a self-consistent way would provide very important information about nuclear matter and its behavior both at zero and at finite temperatures. We could mention in this respect the electron scattering on nuclei [16], the subthreshold particle production [17,18], the calculation of in-medium effective cross sections [4], the backward scattering [19], and of course, a self-consistent calculation of the saturation energy and the properties of the nuclear matter [7,2,8,3,9,11]. In the last example the spectral function is needed not only for the off-shell propagation of nucleons in the ladder diagrams. It enters also in the calculation of the Hartree-Fock energy (through the calculation of the momentum distribution in an interacting system) and the dispersive contribution to the real part of the self-energy. The need for a self-consistent calculation was of course recognized, but real calculation have not been performed, except for restricted kinematical conditions [20]. Only very recently the off-shell nucleon propagation and scattering were addressed [21].

In this work we present an exploratory self-consistent calculation of the nucleon spectral function at finite temperature in the  $T$ -matrix approximation. In the nuclear matter the  $T$ -matrix approximation leads to pairing transition at low temperatures [11,10,9]. We do not intend to address here the superfluidity transition at low temperatures. This means, of course, that we stay at temperatures above the pairing transition. The formalism to treat the pairing in the  $T$ -matrix approximation is still missing both in the quasiparticle as well as in the self-consistent version [10,11]. It should be pointed out that similar self-consistent calculations can be also performed in the Brueckner scheme at low temperatures where no pairing instability occurs.

### II. IN-MEDIUM $T$ MATRIX

In the present work we use the real-time Green's functions formalism [12–14], which we found very suitable for calculations at finite temperature in the Born approximation [6]. In equilibrium the Green's functions are defined by the spectral function:

$$G^<(p, \omega) = if(\omega)A(p, \omega),$$

\*Electronic address: bozek@solaris.ifj.edu.pl

$$G^>(p, \omega) = -i[1 - f(\omega)]A(p, \omega), \quad (1)$$

where

$$f(\omega) = \frac{1}{e^{(\omega - \mu)/T} + 1} \quad (2)$$

is the Fermi distribution and the spectral function  $A$  is

$$A(p, \omega) = -2 \operatorname{Im} G^+(p, \omega). \quad (3)$$

$G^\pm$  denote the retarded (advanced) Green's function. The spectral function can be written equivalently using the self-energy

$$A(p, \omega) = \frac{\Gamma(p, \omega)}{\{[\omega - p^2/2m - \operatorname{Re} \Sigma^+(p, \omega)]^2 + \Gamma(p, \omega)^2/4\}}, \quad (4)$$

where

$$\Gamma(p, \omega) = -2 \operatorname{Im} \Sigma^+(p, \omega). \quad (5)$$

In order to reach a consistent approximation scheme we have to calculate the retarded self-energy  $\Sigma^+$  using the one-particle Green's functions  $G$ . In a previous work we have calculated the self-energy in the Born approximation [6]. Below we address the calculation in the more complicated  $T$ -matrix approximation [12–14]. This approximation takes into account the two-body correlations and thus becomes exact in a dilute system, but is not restricted to zero or low temperatures as the Brueckner approximation. The nuclear matter at normal nuclear density is not a dilute interacting system and corrections from three-body correlations are probably non-negligible. However, the  $T$ -matrix ladder resummation in-medium represents a serious improvement

$$\begin{aligned} \langle \mathbf{p} | \mathcal{G}^\pm(\mathbf{P}, \Omega) | \mathbf{p}' \rangle &= (2\pi)^3 \delta^3(\mathbf{p} - \mathbf{p}') \int \frac{d\omega'}{2\pi} \int \frac{d\omega}{2\pi} \\ &\times \frac{G^<(\mathbf{P}/2 + \mathbf{p}, \omega - \omega') G^<(\mathbf{P}/2 - \mathbf{p}, \omega') - G^>(\mathbf{P}/2 + \mathbf{p}, \omega - \omega') G^>(\mathbf{P}/2 - \mathbf{p}, \omega')}{\Omega - \omega \pm i\epsilon}. \end{aligned} \quad (7)$$

Taking in the above expression only the particle-particle propagator (the  $G^>G^>$  factor) results in the Brueckner approximation. At this point the quasiparticle approximation is usually made

$$A(p, \omega) = 2\pi Z \delta(\omega - \omega_p), \quad (8)$$

where the single-particle energy is the solution of

$$\omega_p = \frac{p^2}{2m} + \operatorname{Re} \Sigma^+(p, \omega_p) \quad (9)$$

and

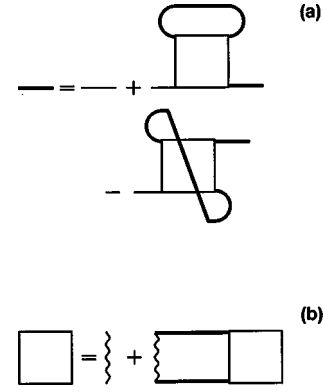


FIG. 1. (a) Diagrammatic representation of the self-energy in the  $T$ -matrix approximation. The self-energy represented in diagram (a) leads to Eqs. (13) and (16). (b) Diagrammatic representation of the  $T$ -matrix equation (6). The thin lines represent the noninteracting fermion propagators, the thick lines are interacting off-shell propagators and the wavy lines denote the interaction potential. In the quasiparticle approximation the in-medium off-shell propagator is replaced by the on-shell propagator in the intermediate states in the  $T$ -matrix equation and in the loops of the self-energy diagrams.

over the Born approximation and gives good approximations for one-particle properties of the system.

The  $T$  matrix (Fig. 1) for a system with a two-body interaction  $V(\mathbf{p}, \mathbf{p}')$  is defined as [12–14]:

$$\begin{aligned} \langle \mathbf{p} | T^\pm(\mathbf{P}, \omega) | \mathbf{p}' \rangle &= V(\mathbf{p}, \mathbf{p}') + \int \frac{d^3k}{(2\pi)^3} \int \frac{d^3q}{(2\pi)^3} V(\mathbf{p}, \mathbf{k}) \\ &\times \langle \mathbf{k} | \mathcal{G}^\pm(\mathbf{P}, \omega) | \mathbf{q} \rangle \langle \mathbf{q} | T^\pm(\mathbf{P}, \omega) | \mathbf{p}' \rangle, \end{aligned} \quad (6)$$

where the disconnected two-particle propagator is

$$Z^{-1} = \left( 1 - \frac{\partial \operatorname{Re} \Sigma^+(p, \omega)}{\partial \omega} \right)_{\omega = \omega_p}. \quad (10)$$

Performing the calculations in the framework of the quasiparticle approximation we shall set, however,  $Z=1$  as has been done in many works [10,3,8]. This results in the on-shell two-particle propagator

$$\langle \mathbf{k} | \mathcal{G}^\pm(\mathbf{P}, \Omega) | \mathbf{k}' \rangle = (2\pi)^3 \delta^3(\mathbf{k} - \mathbf{k}') \frac{1 - f(\omega_{p_1}) - f(\omega_{p_2})}{\Omega - \omega_{p_1} - \omega_{p_2} \pm i\epsilon} \quad (11)$$

with  $\mathbf{p}_{1,2} = \mathbf{P}/2 \pm \mathbf{k}$ . Within the quasiparticle approximation the  $T$ -matrix equation takes the familiar form

$$\begin{aligned} \langle \mathbf{p} | T^\pm(\mathbf{P}, \omega) | \mathbf{p}' \rangle &= V(\mathbf{p}, \mathbf{p}') + \int \frac{d^3k}{(2\pi)^3} V(\mathbf{p}, \mathbf{k}) \\ &\times \frac{1 - f(\omega_{p_1}) - f(\omega_{p_2})}{\omega - \omega_{p_1} - \omega_{p_2} \pm i\epsilon} \langle \mathbf{k} | T^\pm(\mathbf{P}, \omega) | \mathbf{p}' \rangle. \end{aligned} \quad (12)$$

We are using an angular averaged two-particle propagator  $\mathcal{G}^\pm$  both in the the self-consistent equation (6) and in its quasiparticle counterpart (12). This standard approximation for in-medium calculation allows us to perform a partial wave expansion of the  $T$  matrix.

The off-shell propagation of nucleons means that the spectral function is not sharply peaked around  $\omega_p$ , also it cannot be approximated by putting a frequency-independent width  $\Gamma(p)$  in Eq. (4). This implies that the two frequency integrals in Eq. (7) have to be done numerically. The two-particle off-shell propagator  $\mathcal{G}^\pm$  can then be used to calculate the  $T$  matrix using Eq. (6). The equation for the  $T$  matrix is an integral equation, but in the present work we use a separable potential and the solution of Eq. (6) is trivial. However, we make no simplifying assumptions concerning the one-particle spectral functions, so that the intermediate two-particle propagator  $\mathcal{G}^\pm$  takes into account the off-shell nucleon propagation.

The imaginary part of the self-energy can be obtained from the  $T$  matrix

$$\begin{aligned} \text{Im} \Sigma^+(p, \Omega) &= \int \frac{d\omega}{2\pi} \int \frac{d^3k}{(2\pi)^3} A(k, \omega) \\ &\times \langle (\mathbf{p} - \mathbf{k})/2 | \text{Im} T^+(\mathbf{p} + \mathbf{k}, \Omega + \omega) | (\mathbf{p} - \mathbf{k})/2 \rangle_A \\ &\times [f(\omega) + g(\omega + \Omega)], \end{aligned} \quad (13)$$

where the index  $A$  indicates that the  $T$  matrix is antisymmetrized and

$$g(\omega) = \frac{1}{e^{(\omega - 2\mu)/T} - 1} \quad (14)$$

is the Bose distribution. The relation (13) is true at equilibrium. The explicit expressions for the self-energies in the partial wave expansion of the  $T$  matrix can be found, e.g., in [22]. Again in the quasiparticle approximation Eq. (13) simplifies to

$$\begin{aligned} \text{Im} \Sigma^+(p, \Omega) &= \int \frac{d^3k}{(2\pi)^3} \\ &\times \langle (\mathbf{p} - \mathbf{k})/2 | \text{Im} T^+(\mathbf{p} + \mathbf{k}, \Omega + \omega_k) | (\mathbf{p} - \mathbf{k})/2 \rangle_A \\ &\times [f(\omega_k) + g(\omega_k + \Omega)]. \end{aligned} \quad (15)$$

The real part of the self-energy can be obtained using the dispersion relation

$$\text{Re} \Sigma(p, \omega) = \Sigma_{\text{HF}}(p) + \mathcal{P} \int \frac{d\omega'}{2\pi} \frac{\Gamma(p, \omega')}{\omega - \omega'}, \quad (16)$$

where the Hartree-Fock energy is given by

$$\begin{aligned} \Sigma_{\text{HF}}(p) &= -i \int \frac{d\omega}{2\pi} \int \frac{d^3k}{(2\pi)^3} \\ &\times V[(\mathbf{p} - \mathbf{k})/2, (\mathbf{p} - \mathbf{k})/2]_A G^<(k, \omega) \end{aligned} \quad (17)$$

and in the quasiparticle approximation it is

$$\Sigma_{\text{HF}}(p) = \int \frac{d^3k}{(2\pi)^3} V[(p - k)/2, (p - k)/2]_A f(\omega_k). \quad (18)$$

The set of equations (4), (6), (13), and (16) must be solved self-consistently. The numerical solution of this set of equations is done by iteration starting with a spectral function with finite, constant width, and with the Hartree-Fock part of  $\text{Re} \Sigma^+$ . Then the  $T$  matrix is calculated from Eq. (6) and the result is used to obtain the imaginary part of the self-energy from Eq. (13). The iterations are performed until the self-energy becomes stable. Typically around 10 iterations are needed if the starting values of the Fermi energy and the initial value of the single-particle width are of the right order of magnitude.

The quasiparticle approximation in this work means that the  $T$  matrix is calculated from formula (12), where the single-particle energies are determined by the Hartree-Fock energy (18). The  $T$  matrix in the quasiparticle approximation is then used to calculate the imaginary part of the self-energy [Eq. (13)]. The quasiparticle approximation can be improved by calculating the dispersive contribution to the real part of the self-energy [second term in Eq. (16)] [23,11,2,8]. Thus the single-particle energies are modified and the scheme must be iterated until the real part of the self-energy stabilizes. This is, however, still not a self-consistent scheme since the imaginary part of the self-energy is neglected in the calculation of the  $T$  matrix.

### III. SELF-CONSISTENT SPECTRAL FUNCTION

In this section we present the numerical results for the in-medium  $T$  matrix and the nucleon self-energy in the self-consistent calculation and in the quasiparticle approximation. The calculations are performed in a very simple separable rank-one Yamaguchi potential [24]:

$$V(p, p') = \sum_{\alpha} \lambda_{\alpha} g_{\alpha}(p) g_{\alpha}(p') \quad (19)$$

in the  $^1S_0$  and  $^3S_1$  waves, using the form factors

$$g_{\alpha}(p) = \frac{1}{p^2 + \gamma^2}, \quad \gamma = 285.9 \text{ MeV} \quad (20)$$

with  $\lambda_{1S_0} = -0.821 \text{ GeV}^2$  and  $\lambda_{3S_1} = -0.839 \text{ GeV}^2$ . This allows us to relate our results to alternative calculations using the quasiparticle approximation without using a realistic but complicated interaction. We have used a kinematical limit in the momentum integrations, limiting the momentum of any

nucleon to  $|p| < 1200$  MeV, with the grid spacing of around 10 MeV. The effect of the cutoff in the free scattering changes the bounding energy of the deuteron to 2.1 MeV. The energy integrals were performed in the range  $|\omega| < 2400$  MeV with the smallest grid spacing 1.75 MeV at low temperature or for calculations using a preset small single-particle width. In the present version of the calculation we assumed that for all momenta the width of the nucleon spectral functions is sufficiently large so that a direct integration in energies is possible. This limits the calculation to nonzero temperatures, since as small temperatures the single-particle width approaches zero at the Fermi energy like  $T^2$ . Obviously, another limitation comes from the appearance of the pairing instability at small temperatures in the  $T$ -matrix scheme. In practice the lowest possible temperature (using only the  $S$  wave interaction) that we could get stable iterations for is 8 MeV. It is still significantly above the critical temperature for the pairing transition, which is around 4 MeV in the quasiparticle approximation with the assumed interaction [10]. However, the single-particle width obtained at  $T=8$  MeV approaches the spacing grid at the limits of the kinematical region (due to the limitation to  $S$  waves) and near the Fermi momentum (an expected property of an interacting Fermi gas). All the in-medium calculation here presented have been performed at normal nuclear density.

It is easy to notice that the generalization of the  $T$ -matrix calculation to include off-shell intermediate nucleon propagators does not change qualitatively the fact that a pairing instability appears at some critical temperature. The imaginary part of the  $T$  matrix with off-shell propagators also vanishes at  $\omega = 2\mu$  and at some temperature a pole appears in the real part of the  $T$  matrix. As mentioned above we could not study numerically the vicinity of the critical temperature in the self-consistent calculation.

In Fig. 2 the imaginary part of the self-energy at zero momentum is given for different temperatures as a function of energy. In all the cases the self-consistent results are very different from the quasiparticle approximation. The self-consistent self-energies having generally a smaller imaginary part. As the temperature is lowered more structure is visible in the self-energy. Beyond the minimum at the Fermi energy ( $\mu \approx -21$  MeV at  $T=10$  MeV) a second maximum appears around the energy  $2\mu - \omega_0$ , both in the self-consistent and in the quasiparticle approximation.

The quasiparticle approximation, in the version here presented, is using Hartree-Fock single-particle energies. This can be improved by defining the real-part of the self-energy self-consistently from the  $T$  matrix. The quasiparticle single-particle energies can then be obtained from Eq. (9). We assumed also that the strength of the quasiparticle pole is  $Z = 1$ . It is known that in the Brueckner scheme second and third-order rearrangement terms include corrections to the real part of the self-energy and to the pole strength [23]. In the  $T$ -matrix calculation these corrections were estimated iteratively [3,23]. We can test if these corrections can account for the difference between the quasiparticle and the self-consistent calculation. To this effect we shall use the real-part of the self-energy and the pole strength  $Z$  obtained from the self-consistent calculation together with a small constant width in the spectral function. In Fig. 2 for  $T=10$  MeV the dashed line represents the imaginary part of the self-energy

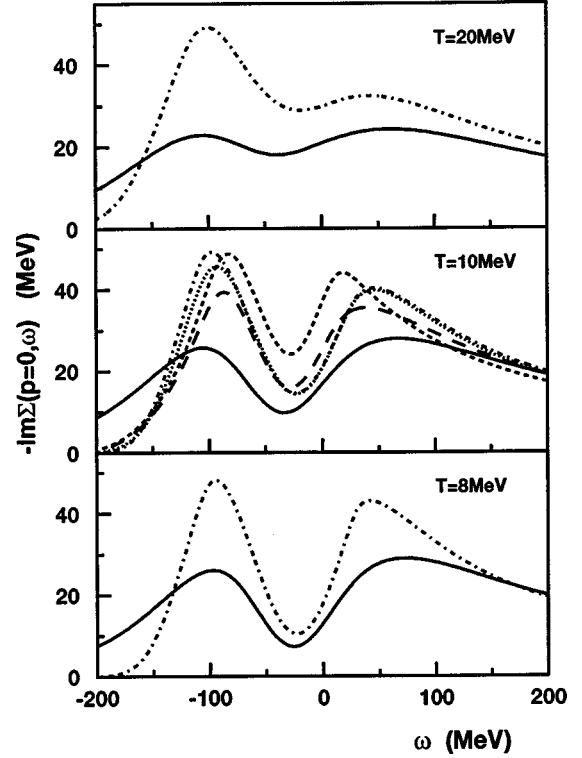


FIG. 2. The imaginary part of the retarded self-energy as a function of energy for  $p=0$  at normal nuclear density and at different temperatures. The solid lines denote the self-consistent self-energies and the dashed-dotted lines denote the results of the quasiparticle approximation. For  $T=10$  MeV the dotted line denotes the result when taking the Hartree-Fock energy as the real part of the self-energy and a constant width of the spectral function of 6 MeV. The dashed line denotes the result of taking the self-consistent real part of the self-energy but a constant width of 6 MeV in the imaginary part of the self-energy. The long-dashed line represents the result, when taking in addition the renormalization factor  $Z$  from the self-consistent solution.

obtained using the same real part of the self-energy as in the self-consistent solution but with the imaginary part of the self-energy fixed at 6 MeV. The small width of the spectral function mimics in that case the  $\delta$  function of the spectral function in the quasiparticle approximation. The resulting  $\text{Im} \Sigma^+$  is again very different from the self-consistent solution. We have also taken into account the effect of the renormalization factor  $Z$  and of the shift in the real part of the self-energy in the quasiparticle-spectral function together. The result (long-dashed line for  $T=10$  MeV in Fig. 2) is closer to the self-consistent solution than other quasiparticle approximations. The  $Z$  factor is smaller than 1 close to the Fermi energy, reducing the occupancies for states contributing the most to the scattering width. It explains why this result is closer to the self-consistent one. However, it is still significantly different. It proves that it is not sufficient to take into account the correct real part of the self-energy and the correct strength of the quasiparticle peak (the same as in the self-consistent solution) and to neglect the imaginary part of the self-energy. The full spectral function for the nucleon with momentum- and frequency-dependent single-particle width must be taken for the intermediate propagators in the  $T$ -matrix equation (6). For  $T=10$  MeV we plot also the re-

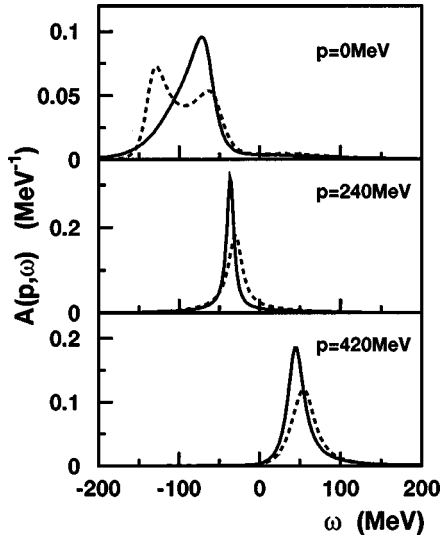


FIG. 3. The nucleon spectral function as a function of energy at normal nuclear density and at  $T=10$  MeV for three different momenta. The solid and the dashed lines denote the self-consistent and the quasiparticle approximation results, respectively.

sult obtained by taking only the Hartree-Fock self-energy for the real part of the self-energy, i.e., the same as in the quasiparticle approximation and a constant width in the spectral function of 6 MeV. The result is very close to the one obtained in the quasiparticle approximation, meaning that a spectral function of width 6 MeV can be approximated by a  $\delta$  function. However, the true spectral function is different and cannot be taken as a  $\delta$  function.

The differences in the imaginary part of the self-energy lead to significant differences in the spectral function. In Fig. 3 the spectral functions are plotted for the quasiparticle and the self-consistent calculations. These results demonstrate that the nucleon spectral function cannot be calculated in the quasiparticle approximation. The position of the quasiparticle peak is different in the two calculation. It is due to differences in the real part of the self-energy. The Hartree-Fock energies are slightly different because of different momentum distributions. Also the dispersive contribution to the real part of the self-energy are different because they originate from very different imaginary parts of the self-energies in the two calculations. However, not only the positions of the peaks in the spectral functions are different, also their widths and shapes are different. Improvements on the calculation of the real part of the self-energy will not lead to a correct spectral function as long as the proper width of the intermediate propagators in the  $T$ -matrix equation is not taken into account, giving the correct self-consistent real *and* imaginary parts of the self-energy.

In Fig. 4 the imaginary part of the self-energy at the quasiparticle pole as a function of momentum is given. The decrease of the single-particle width with the temperature and a minimum around the Fermi energy can be observed. In Fig. 5 the Hartree-Fock energy and the complete real part of the self-energy at the quasiparticle pole in the self-consistent calculation, and the Hartree-Fock energy in the quasiparticle approximation are given as a function of momentum. The behavior of the real part of the self-energy at the temperatures studied is relatively smooth. Only at the lowest tem-

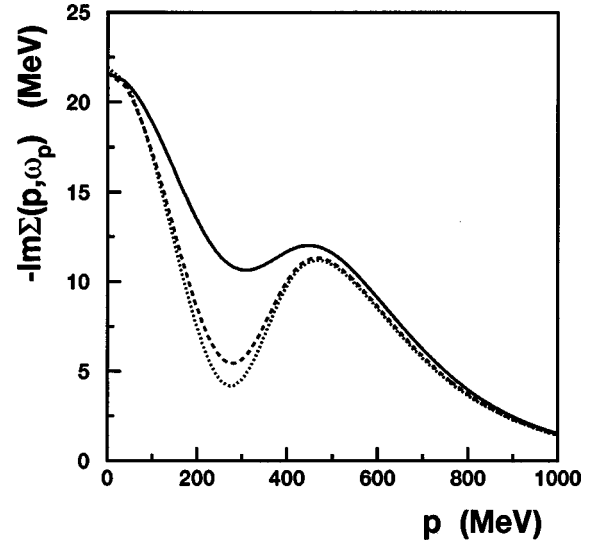


FIG. 4. The imaginary part of the retarded self-energy at the quasiparticle pole as a function of momentum at normal nuclear density. All the results are for the self-consistent calculation. The solid, dashed, and dotted lines represent  $\text{Im} \Sigma^+$  at 20, 10, and 8 MeV, respectively.

perature  $T=8$  MeV does a wiggle start to appear similar to the one observed in [10]. The momentum distributions are more diffuse for off-shell nucleons, leading to smoother dependence of the Hartree-Fock energy on momentum than in the quasiparticle approximation [10]. The difference between the single-particle energies in the self-consistent calculation and in the quasiparticle approximation (dotted and dashed lines in Fig. 5), leads to very different scattering width also when using the same imaginary part of the self-energy (dotted and dashed lines in Fig. 2).

To close this section we would like to make one observation concerning the behavior of the self-energy around the

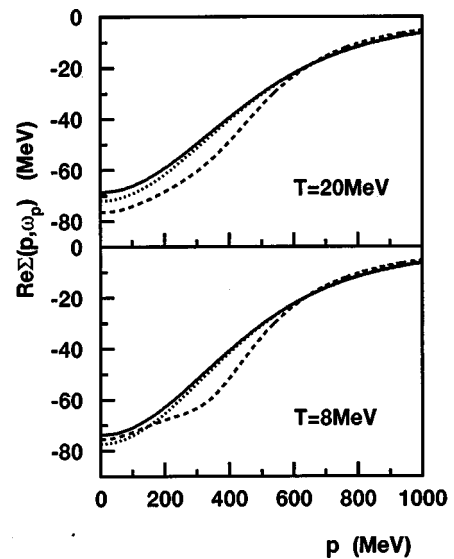


FIG. 5. The Hartree-Fock energy in the self-consistent calculation (solid line) and in the quasiparticle approximation (dotted line) and the real part of the retarded self-energy in the self-consistent calculation on shell (dashed line) as functions of momentum at normal nuclear density and at temperatures of 20 and 8 MeV.

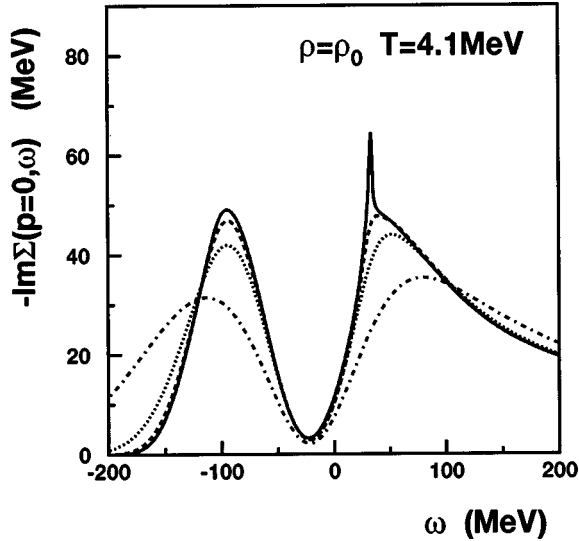


FIG. 6. The imaginary part of the retarded self-energy as function of energy for  $p=0$  at normal nuclear density and  $T=4.1$  MeV. The solid line denotes the quasiparticle approximation and the dashed, dotted, and dashed-dotted lines represent the results obtained using a fixed single-particle width of 6, 15, and 40 MeV, respectively.

pairing transition. At the critical temperature of the pairing transition a pole appears in the  $T$  matrix for pairs with zero total momentum both in the self-consistent and in the quasiparticle calculations. In the quasiparticle approximation it leads to a singularity in the imaginary part of the self-energy [10]. In the calculation of the self-energy using the off-shell propagators (13) there is one more energy integration which washes out this singularity. As an illustration we show in Fig. 6 the imaginary part of the self-energy at  $T$

$=4.1$  MeV in the quasiparticle approximation, compared to results obtained using a fixed width of the spectral function and the same Hartree-Fock energy as in the quasiparticle calculation. We observe that the singularity which starts to build up at  $T=4.1$  MeV in the quasiparticle approximation is no longer present if finite widths of propagators are taken. Note that it is the off-shellness of the propagator in the calculation of the self-energy (13) not in the  $T$ -matrix equation, which causes the singularity in  $\text{Im} \Sigma^+$  to disappear.

#### IV. IN-MEDIUM CROSS SECTIONS

The modeling of the nonequilibrium evolution in a heavy-ion reaction by semiclassical transport models requires the knowledge of the in-medium cross section. For nucleons on-shell one can define the scattering cross sections similarly as in vacuum, but using an effective mass [4]. If the nucleons are off-shell the definition of the cross section must be modified because the outgoing waves are localized in space [21]. In this section we will use a simplistic view of the scattering cross section as a parameter in the semiclassical collision integral. The applicability of the quasiparticle approximations in the description of the nonequilibrium dynamics is questionable if the equilibrium calculations indicate the need for self-consistent off-shell calculations. However, in order for the complex dynamical evolution to be tractable we have to restrict ourselves to quasiparticle transport models of heavy-ion collisions. One can, however, take into account in-medium modifications of the effective cross sections. In particular when calculating the in-medium cross sections at equilibrium one can take into account the full propagators in the ladder diagrams.

The semiclassical collision term for a nucleon of momentum  $p_1$  and energy  $\omega_1$  has the form [13]

$$\int \frac{d\omega_2}{2\pi} \frac{d^3p_2}{(2\pi)^3} \int \frac{d\omega_3}{2\pi} \frac{d^3p_3}{(2\pi)^3} \int \frac{d\omega_4}{2\pi} \frac{d^3p_4}{(2\pi)^3} (2\pi)^4 \delta^3(\mathbf{p}_1 + \mathbf{p}_2 - \mathbf{p}_3 - \mathbf{p}_4) \delta(\omega_1 + \omega_2 - \omega_3 - \omega_4) \\ \times |\langle \mathbf{k} | T^+(\mathbf{P}, \omega_1 + \omega_2) | \mathbf{k}' \rangle_A|^2 A(\mathbf{p}_1, \omega_1) A(\mathbf{p}_2, \omega_2) A(\mathbf{p}_3, \omega_3) \{ [1 - f(\mathbf{p}_1, \omega_1)] [1 - f(\mathbf{p}_2, \omega_2)] f(\mathbf{p}_3, \omega_3) f(\mathbf{p}_4, \omega_4) \\ - f(\mathbf{p}_1, \omega_1) f(\mathbf{p}_2, \omega_2) [1 - f(\mathbf{p}_3, \omega_3)] [1 - f(\mathbf{p}_4, \omega_4)] \}, \quad (21)$$

where  $\mathbf{P} = \mathbf{p}_1 + \mathbf{p}_2$ ,  $\mathbf{k} = (\mathbf{p}_1 - \mathbf{p}_2)/2$ ,  $\mathbf{k}' = (\mathbf{p}_3 - \mathbf{p}_4)/2$ . When putting the scattering particles on-shell and integrating over the angle<sup>1</sup> we can define an effective cross section  $\sigma$  in the collision term

$$\int \frac{d^3p_2}{(2\pi)^3} \frac{|\mathbf{p}_1 - \mathbf{p}_2|}{M^*(P, k)} \sigma \{ [1 - f(\mathbf{p}_1)] [1 - f(\mathbf{p}_2)] f(\mathbf{p}_3) f(\mathbf{p}_4) \\ - f(\mathbf{p}_1) f(\mathbf{p}_2) [1 - f(\mathbf{p}_3)] [1 - f(\mathbf{p}_4)] \}, \quad (22)$$

where

$$M^*(P, k) = \left( \frac{\partial \langle \omega_{p_1} + \omega_{p_2} \rangle_\Omega}{\partial k^2} \right)^{-1} \quad (23)$$

is the effective mass. The sign  $\langle \dots \rangle_\Omega$  denotes the averaging over the angle. The cross section is

$$\sigma(P, k) = \frac{M^*(P, k)^2}{4\pi} \langle |\langle \mathbf{k} | T^+(P, \omega_{p_1} + \omega_{p_2}) | \mathbf{k} \rangle_A|^2 \rangle_\Omega. \quad (24)$$

In Fig. 7 are presented the results for the  $n$ - $p$  and  $n$ - $n$  cross sections. The in-medium cross sections calculated with the self-consistent  $T$  matrix are generally larger than the cross sections obtained in the framework of the quasiparticle

<sup>1</sup>We use only the  $S$  wave in the present work.

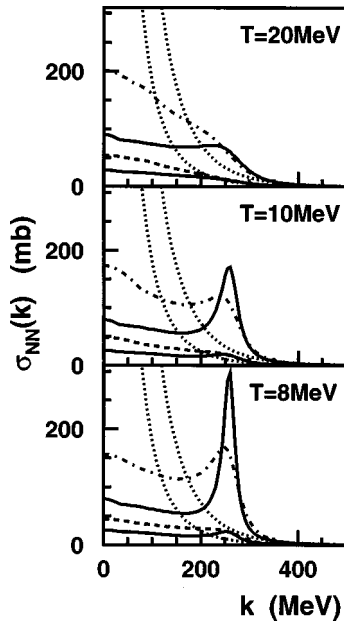


FIG. 7. The in-medium cross sections for the scattering of on-shell quasiparticles with zero total momentum as functions of the c.m. momentum at three different temperatures and at normal nuclear density. The dashed-dotted and the dashed lines denote the  $n$ - $p$  and the  $n$ - $n$  cross sections, respectively, calculated with the self-consistent in-medium  $T$  matrix. The solid lines denote the corresponding in-medium cross sections calculated with the  $T$  matrix in the quasiparticle approximation and the dotted lines represent the corresponding free cross sections.

approximation. Only part of the difference can be explained by a factor originating in the difference in the effective masses in the two calculations. Both cross sections present a resonancelike peak in the  $n$ - $p$  scattering related to the pairing resonance (above  $T_c$ ). These kind of structures in the energy dependence of the cross sections do not influence the evolution of the system, since the cross sections are always integrated over momentum [25]. However, the overall average cross sections in Fig. 7 are different and could lead to different transport properties in the collision. Before definite conclusions can be drawn calculations should be repeated with a realistic interaction.

## V. CONCLUSIONS

We have presented a self-consistent calculation of the in-medium  $T$  matrix. The intermediate propagators in the

$T$ -matrix equation are full off-shell propagators. Both the real and imaginary part of the self-energy in these propagators have been obtained consistently from the  $T$  matrix. The coupled system of equations was solved by iteration for the case of a simple separable interaction. The results were compared to a calculation using the quasiparticle approximation for the intermediate propagators in the  $T$ -matrix equation.

The imaginary parts of the self-energies and the spectral functions obtained in the two calculations are very different. One cannot calculate reliably the spectral functions without using consistently the same spectral function through the whole approximation scheme. The width of the self-consistent spectral function is generally smaller than its quasiparticle estimates. The self-consistent  $T$  matrix also presents a pairing instability at some critical temperature. However, in the vicinity of the critical temperature the self-consistent iteration procedure cannot be performed numerically.

We have calculated the corresponding in-medium cross sections in the two approximations. The obtained cross sections are different and indicate that a self-consistent resummation of the ladder diagrams may be important for a correct estimation of transport properties of the nuclear matter at finite temperature.

The spectral functions are very sensitive to approximations of the imaginary part of the propagators in the  $T$ -matrix equation. In the present work we have demonstrated both the necessity and the feasibility of a full self-consistent ladder diagram resummation when calculating the spectral functions in the nuclear matter at finite temperature. The method here presented could also be applied to Brueckner-type calculations. Before applying the iteration procedure to zero or low temperature, an explicit method of energy integration for quasiparticles around the Fermi energy must be implemented. Similar methods must be used to overcome the limitations in the momenta of nucleons due to the cutoff. Nucleons with large momenta are important for the description of short-range correlations. Since generally the width of the spectral function is smaller at low temperature, one may expect that the effect of the off-shell nucleon propagation would be less dramatic at zero temperature.

## ACKNOWLEDGMENTS

The author is grateful to Paweł Danielewicz for enriching discussions. He would also like to thank the NSCL for hospitality. This work was partly supported by the National Science Foundation under Grant No. PHY-9605207.

- 
- [1] A. L. Fetter and J. D. Walecka, *Quantum Theory of Many-Particle Systems* (McGraw-Hill, New York, 1971).
  - [2] M. Baldo, I. Bombaci, G. Giansiracusa, U. Lombardo, C. Mahaux, and R. Sator, Nucl. Phys. **A545**, 741 (1992).
  - [3] H. S. Köhler, Phys. Rev. C **46**, 1687 (1992).
  - [4] G. Q. Li and R. Machleidt, Phys. Rev. C **48**, 1702 (1993); H.-J. Schulze, A. Schnell, G. Röpke, and U. Lombardo, *ibid.* **55**, 3006 (1997); A. Schnell, G. Röpke, U. Lombardo, and H.-J. Schulze, *ibid.* **55**, 806 (1998).
  - [5] J. Knoll and N. Voskresenskii, Phys. Lett. B **351**, 43 (1995); Ann. Phys. (N.Y.) **249**, 532 (1996).
  - [6] P. Bozek, in *Proceedings of the I-V Workshop on Nonequilibrium Physics at Short Time Scales*, edited by K. Morawetz, P. Lipavský, and V. Špička (Universität Rostock, Rostock, 1998).
  - [7] O. Benhar, A. Fabrocini, and S. Fantoni, Nucl. Phys. **A550**, 201 (1992).
  - [8] B. E. Vonderfecht, W. H. Dickhoff, A. Polls, and A. Ramos, Nucl. Phys. **A555**, 1 (1993).

- [9] B. E. Vonderfecht, W. H. Dickhoff, A. Polls, and A. Ramos, *Phys. Rev. C* **44**, R1265 (1991).
- [10] T. Alm, G. Röpke, A. Schnell, N. H. Kwong, and S. Köhler, *Phys. Rev. C* **53**, 2181 (1996).
- [11] A. Schnell, T. Alm, and G. Röpke, *Phys. Lett. B* **387**, 443 (1996).
- [12] L. P. Kadanoff and G. Baym, *Quantum Statistical Mechanics* (Benjamin, New York, 1962).
- [13] P. Danielewicz, *Ann. Phys. (N.Y.)* **152**, 239 (1984).
- [14] W. Botermans and R. Malfliet, *Phys. Rep.* **198**, 115 (1990).
- [15] P. Danielewicz, *Ann. Phys. (N.Y.)* **152**, 305 (1984).
- [16] S. Boffi, C. Gusti, F. Pacati, and M. Radici, in *Electromagnetic Response of Atomic Nuclei* (Clarendon, Oxford, 1996); J. J. Kelly, in *Advances in Nuclear Physics*, Vol. 23, edited by J. W. Negele and E. W. Vogt (Plenum, New York, 1996); A. Polls, M. Radici, S. Boffi, W. H. Dickhoff, and H. Müther, *Phys. Rev. C* **55**, 810 (1997).
- [17] W. Cassing, V. Metag, U. Mosel, and K. Niita, *Phys. Rep.* **188**, 363 (1990).
- [18] P. Božek, *Phys. Rev. C* **56**, 1452 (1997).
- [19] P. Danielewicz, *Phys. Rev. C* **42**, 1564 (1990).
- [20] R. Rapp and J. Wambach, *Phys. Lett. B* **315**, 220 (1993).
- [21] W. H. Dickhoff, *Phys. Rev. C* **58**, 2807 (1998).
- [22] M. Schmidt, G. Röpke, and H. Schulz, *Ann. Phys. (N.Y.)* **202**, 57 (1990).
- [23] H. S. Köhler and R. Malfliet, *Phys. Rev. C* **48**, 1034 (1993).
- [24] Y. Yamaguchi, *Phys. Rev.* **95**, 1628 (1954).
- [25] T. Alm, G. Röpke, W. Bauer, F. Daffin, and M. Schmidt, *Nucl. Phys.* **A587**, 815 (1995).